Cell PRESS
Neuron
Article

Glycinergic Transmission Shaped by the Corelease of GABA in a Mammalian Auditory Synapse

Tao Lu,[1,*] Maria E. Rubio,[2] and Laurence O. Trussell[1]
[1]Oregon Hearing Research Center and Vollum Institute, Oregon Health & Science University, Portland, OR 97239, USA
[2]Department of Physiology and Neurobiology, University of Connecticut, Storrs, CT 06269, USA
*Correspondence: lut@ohsu.edu
DOI 10.1016/j.neuron.2007.12.010

SUMMARY

The firing pattern of neurons is shaped by the convergence of excitation and inhibition, each with finely tuned magnitude and duration. In an auditory brainstem nucleus, glycinergic inhibition features fast decay kinetics, the mechanism of which is unknown. By applying glycine to native or recombinant glycine receptors, we show that response decay times are accelerated by addition of GABA, a weak partial agonist of glycine receptors. Systematic variation in agonist exposure time revealed that fast synaptic time course may be achieved with submillisecond exposures to mixtures of glycine and GABA at physiological concentrations. Accordingly, presynaptic terminals generally contained both transmitters, and depleting terminals of GABA slowed glycinergic synaptic currents. Thus, coreleased GABA accelerates glycinergic transmission by acting directly on glycine receptors, narrowing the time window for effective inhibition. Packaging both weak and strong agonists in vesicles may be a general means by which presynaptic neurons regulate the duration of postsynaptic responses.

INTRODUCTION

Glycine is the major inhibitory transmitter in the lower auditory pathway; glycinergic interneurons and projection neurons modify the response to acoustic stimuli from the cochlear nucleus to the inferior colliculus. The temporal precision of inhibition is critical for circuits involved in sound localization (Awatramani et al., 2004; Brand et al., 2002; Tollin, 2003). Recent studies have shown that glycinergic inhibition is mediated by extremely brief synaptic responses, with submillisecond decay times in mature synapses at physiological temperature (Awatramani et al., 2004, 2005; Magnusson et al., 2005), briefer than those reported at other glycinergic synapses (Chéry and de Koninck, 1999; Dugué et al., 2005; Singer and Berger, 1999).

GABA and glycine are coexpressed by many neurons in the brainstem, cerebellum, and spinal cord (Dugué et al., 2005; Ostapoff et al., 1997; Rubio and Juiz, 2004; Todd and Sullivan, 1990; Wenthold et al., 1987) and are packaged into synaptic vesicles by the same transporter, VIAAT, indicating that the two transmitters are coreleased (Chaudhry et al., 1998; Sagné et al., 1997; Wojcik et al., 2006). Although this coexpression disappears with age in some brain regions (Muller et al., 2006; Nabekura et al., 2004), it does persist into adulthood in a wide variety of cell types (Gleich and Vater, 1998; Korada and Schwartz, 1999; Moore et al., 1996; Ostapoff et al., 1997; Riquelme et al., 2001; Rubio and Juiz, 2004; Spirou and Berrebi, 1997; Wenthold et al., 1987). However, the function of corelease remains unclear, and indeed transmission at many such synapses is mediated largely by postsynaptic glycine receptors (Chéry and de Koninck, 1999, 2000; Lim et al., 2000; Wu and Oertel, 1986).

It is generally believed that fast-acting neurotransmitters reach millimolar levels in the synaptic cleft for brief periods of time and that the decay of the postsynaptic response reflects the intrinsic gating kinetics of the channels as transmitter unbinds and leaves the cleft (Clements et al., 1992; Overstreet et al., 2002). We show here that GABA at physiological concentrations speeds the decay of glycine responses in membrane patches from the medial nucleus of the trapezoid body (MNTB). The glycinergic boutons in MNTB generally contained GABA, and depleting such terminals of GABA slowed the decay time of glycine receptor-mediated synaptic currents. Thus, the function of corelease may be to enhance the temporal precision of inhibition.

RESULTS

Responses to Glycine in Membrane Patches

In rat MNTB, glycinergic terminals generate inhibitory postsynaptic currents (IPSCs) that are completely blocked by 0.5 μM strychnine (Awatramani et al., 2004). In P9–11 rats, miniature inhibitory postsynaptic currents (mIPSCs), each activated by the spontaneous release of a single synaptic vesicle, sometimes have mixed components generated by both glycine and $GABA_A$ receptors, indicating corelease (Awatramani et al., 2005). Although these mIPSCs with mixed components disappear with age, GABA may still be coreleased with glycine. GABA is a weak, partial agonist of glycine receptors (De Saint Jan et al., 2001; Lewis et al., 2003). If coreleased with glycine, GABA might alter the properties of the glycine receptor and thus shape glycinergic transmission. We tested this hypothesis by excising patches of MNTB membrane from P10–18 rats and applying glycine with and without GABA, comparing the responses to synaptic currents. Rise times (10%–90%) to 1 mM glycine applied for

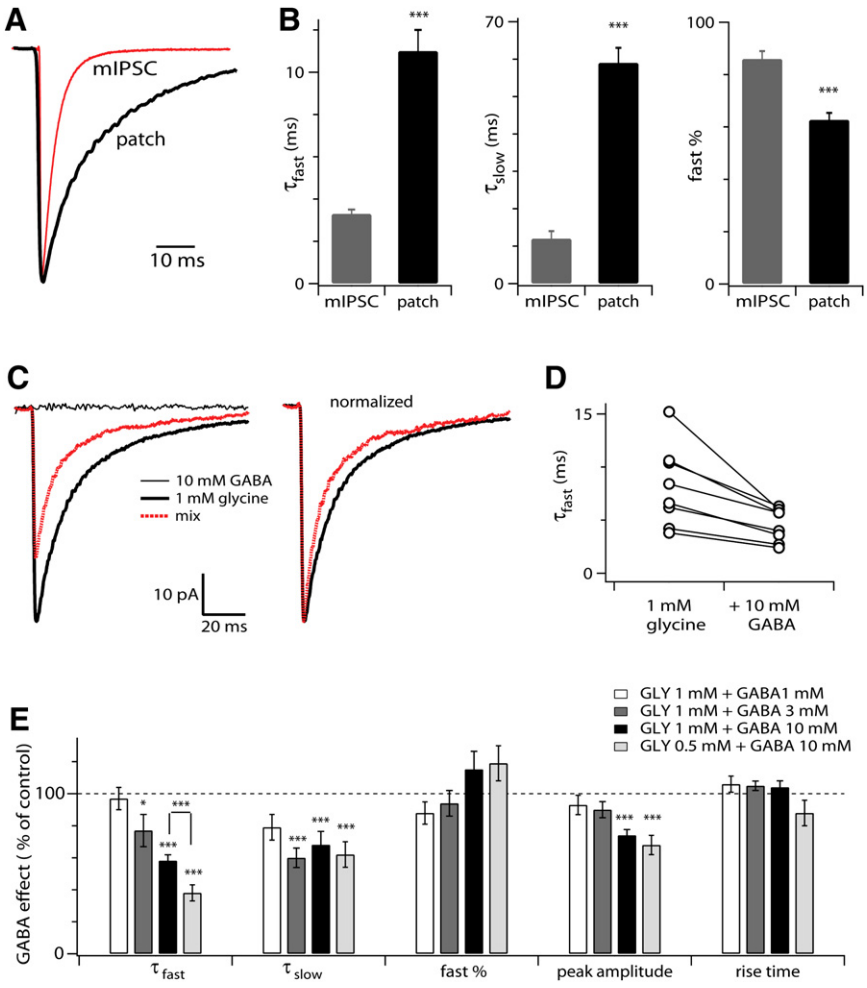

Figure 1. GABA Modifies the Kinetics and Amplitude of Patch Responses to Glycine in MNTB

(A) Normalized mIPSC (average of 300 events) and patch response to 1 ms pulse of 1 mM glycine (average of 20 applications to a patch excised from the same cell). Recorded in the presence of 20 μM SR95531.

(B) Summary of decay kinetics of mIPSCs (n = 13) and patch responses to 1–3 mM glycine for 1 ms (n = 40). Significant difference existed for each kinetic parameter between the synaptic and patch responses ($p < 0.001$).

(C) The left panel shows the responses of one MNTB patch to 1 ms application of 1 mM glycine, 10 mM GABA, or a mix of both. $GABA_A$ receptors were blocked with 20 μM SR-95531. Each trace was the average of 10 to 20 repetitions. Peak amplitude of the glycine response was reduced by about 25% with the inclusion of GABA. The acceleration in decay was evident when the responses were normalized (right panel).

(D) GABA shortened the τ_{fast} of the glycine response in all seven patches using 1 mM glycine and 10 mM GABA.

(E) The effects of different concentrations of GABA and glycine applied with 1 ms pulses. Data were normalized and statistically tested against values with glycine alone (n = 3–10 patches).

Error bars indicate ± SEM.

1 ms were 0.76 ± 0.03 ms (n = 14) and to 0.5 mM glycine were 1.04 ± 0.12 ms (n = 9). mIPSCs rose in 0.32 ± 0.01 (n = 13), suggesting larger and/or briefer synaptic glycine transients than that used on the patch. The patch response to glycine alone (1–3 mM; 1 ms pulse) decayed biexponentially with a τ_{fast} = 11 ± 1 ms, τ_{slow} = 56 ± 5 ms, and fast%, the percent contribution to peak response by the fast component, was 60% ± 5% (n = 40 patches; Figures 1A and 1B). By contrast, glycine receptor-mediated mIPSCs were much briefer, decaying biexponentially with a τ_{fast} of 3.3 ± 0.2 ms (fast component 86% ± 3%) and a τ_{slow} of 12 ± 2 ms (n = 13 cells; Figures 1A and 1B). While time constants in patches varied widely, perhaps an effect of receptor density on affinity (De Saint Jan et al., 2001), only 2 of 40 patches had a τ_{fast} similar to that of mIPSCs. This discrepancy has been previously noted in other mammalian systems (Harty and Manis, 1998; Singer and Berger, 1999). Control experiments explored the possibility that receptors in patches are altered as a consequence of excision or do not represent the synaptic population. However, the decay kinetics were not significantly faster for patches taken from cells with synapses enzymatically stripped off, which makes synaptic receptors more available for study, or from nucleated patches, which better preserves cytosolic components that regulate receptors (see Figure S1B available online). Inclusion of phalloidin in the pipette (Singer and Berger, 1999), allowing it to diffuse into the cell prior to patch excision, had no effect on response kinetics (Figure S1B). Moreover, decay kinetics were unchanged when glycine was rapidly applied to isolated whole cells (Figure S1), thus excluding the possibility that cells contain populations of fast, synaptic receptors that may not be probed by our excised patch technique. Finally, we examined deactivation as a function of glycine concentration (Figure S1C), finding significantly faster deactivation only for 0.1 mM glycine, a concentration well below the EC_{50} of the receptor using brief pulses (Jonas et al., 1998; Singer and Berger, 1999).

Zn^{2+} is an endogenous modulator of glycinergic signals (Smart et al., 2004; Suwa et al., 2001). Since responses of patches and synapses might differ because of differences in ambient Zn^{2+} levels (Suwa et al., 2001), we examined the effect of chelation or application of this ion. However, chelation of Zn^{2+} with 5–10 mM tricine did not alter mIPSC decays (91% ± 8% of control, p = 0.31, n = 6 cells), nor did application of 1 μM free Zn^{2+} (10 mM tricine plus 250 μM Zn^{2+}; 87% ± 4% of that in tricine alone, p = 0.08, n = 3; Suwa et al., 2001). Taken together, the data described above indicate that the differences between patch and synaptic glycine receptors cannot be accounted for by artifacts in the patch technique or lack of modulators.

However, patch decay kinetics were accelerated when glycine was coapplied with millimolar levels of GABA (Figure 1C). These concentrations of GABA were chosen because modeling studies

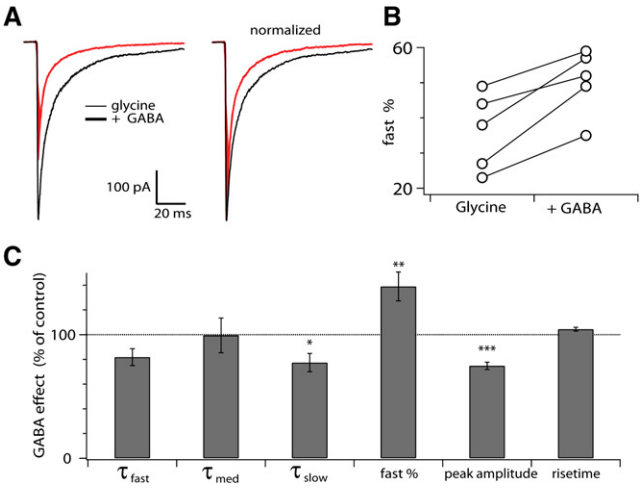

Figure 2. GABA Modifies the Glycine Response of Homomeric α1 Glycine Receptors

(A) The responses of a patch pulled from a HEK293 cell expressing homomeric α1 receptors to 1 ms application of 1 mM glycine, with or without 10 mM GABA (left panel, averages of four to six applications). The addition of GABA reduced the peak amplitude by one-third and accelerated the decay (right panel, normalized traces).

(B) Fast%, the contribution of fast component to peak response, for α1 receptors was increased with the addition of GABA in all five patches tested.

(C) Unlike for MNTB glycine receptors, the fast %, but not the τ_{fast}, for α1 receptors was significantly affected by mixing 10 mM GABA with 1 mM glycine. Moreover, GABA produced a significant reduction in τ_{slow} and peak amplitude (n = 5).

Error bars indicate ± SEM.

have suggested that the peak levels in the synaptic cleft may be between 1 and 10 mM (Overstreet et al., 2002). As shown in Figures 1C–1E, GABA significantly accelerated the τ_{fast} and τ_{slow} of the patch response, with only a modest reduction in peak amplitude and no effect on rise time. Consistent with a competition between these two agonists, greater acceleration was seen with greater GABA/glycine ratio (Figure 1E). Mixtures of 0.5 mM glycine plus 10 mM GABA gave the briefest decays, but significant effects were seen even with 1 mM glycine plus 3 mM GABA. These effects of GABA were not due to contamination by $GABA_A$ receptor responses, as they were recorded in the presence of the $GABA_A$ receptor antagonist SR-95531 (20 μM). Moreover, GABA alone induced no response in this condition (Figure 1C), and all responses were completely blocked with 1 μM strychnine (data not shown).

Postsynaptic glycine receptors in MNTB are most likely α1-β heteromers (Friauf et al., 1997; Leao et al., 2004). We tested the effect of GABA on patches from HEK293 cells expressing homomeric glycine receptors consisting of α1 subunits, the glycine-binding subunit prevalent at most mature glycinergic synapses. Here, GABA also sped up the decay and reduced the peak amplitude of glycine responses (Figure 2A), confirming that the activation of $GABA_A$ receptors is not required. Possibly because of the different subunit composition, the effect of GABA on kinetic parameters of decay was different from that in MNTB; GABA significantly increased fast% and reduced τ_{slow} (Figurse 2B and 2C). Thus, by acting as a coagonist, GABA accelerates the kinetics of the glycine receptor.

Although patches responded significantly faster with GABA plus glycine, the fast decay constant still did not match the synaptic waveform in MNTB. This discrepancy probably resulted from the differences in glycine exposure time in patches versus the synaptic cleft. When 1 mM glycine was applied for varying durations, the decay of current following its removal was slower for longer applications, even though the actual removal time was identical (Figure 3A). On average, with a 2 ms application, τ_{fast} was 10.6 ± 0.9 ms (n = 26), while for a 200 μs pulse, the τ_{fast} was 5.7 ± 0.5 ms (n = 16, p = 0.0002; Figure 3C). When this relation was constructed with a mixture of glycine and GABA, we found that for applications of 1 ms or less, 3 mM GABA significantly shortened the fast and slow τs compared to glycine alone (Figures 3B–3D, $p < 0.05$), while 10 mM GABA had a still larger effect. Figure 3E shows that the 200–250 μs application of 10 mM GABA paired with 1 mM glycine gave a τ_{fast} that was faster than mIPSCs (2.5 ± 0.3 ms, n = 14, p = 0.04), while 3 mM GABA plus 1 mM glycine gave a τ_{fast} indistinguishable from synaptic decay times for this age range (3.4 ± 0.5 ms, n = 14, p = 0.79). As expected, shortening the exposure time reduced the rise times sufficiently (0.36 ± 0.02 ms, n = 26 for 0.2–0.25 ms application, pooled from all patches with 1 mM glycine), not different from synaptic rise times (p = 0.14). Together, these data suggest that very rapid glycinergic signaling may arise from coexposure of receptors to glycine and GABA for a submillisecond period. We emphasize that this particular combination of glycine/GABA ratio and exposure duration resulting in synaptic-like fast time constants is probably one of a spectrum of values: for example, lowering the GABA level combined with even shorter pulses might give similar results. However, in the following two sections we demonstrate the presence of presynaptic GABA and its effectiveness in shaping the IPSC.

Immunolocalization of Transmitters in Boutons

Are these transmitters coreleased in the MNTB? Although mixed GABAergic and glycinergic transmission was previously demonstrated for a fraction of terminals in MNTB from P9–11 rats, IPSCs in older animals were generally glycinergic (Awatramani et al., 2005). It is likely, however that GABA continues to be released. Postembedding immuno-EM was used to localize GABA and glycine in boutons on MNTB at P10 and P16. GABA primary antibodies were labeled with secondary antibodies conjugated to 10 nm gold particles, while glycine was detected using secondary antibodies conjugated to 5 nm gold particles. Synaptic endings colabeled with GABA and glycine were observed on the cell body and dendrites of MNTB neurons at both ages (Figure 4, see also Figure S2). These endings made symmetric synaptic contacts, contained pleomorphic synaptic vesicles, and were clearly distinguishable from endings containing flattened synaptic vesicles that labeled only for glycine. The glutamatergic calyx of Held on MNTB cell bodies lacked gold particles for either GABA or glycine (Figure S3). As shown in Figure 5, the percent of endings containing both transmitters was 51% at P10 and 68% at P16, with solely glycine-containing synapses comprising 44% and 30%, respectively, of the terminals. At the antibody concentration we used, the density of glycine particles was similar in

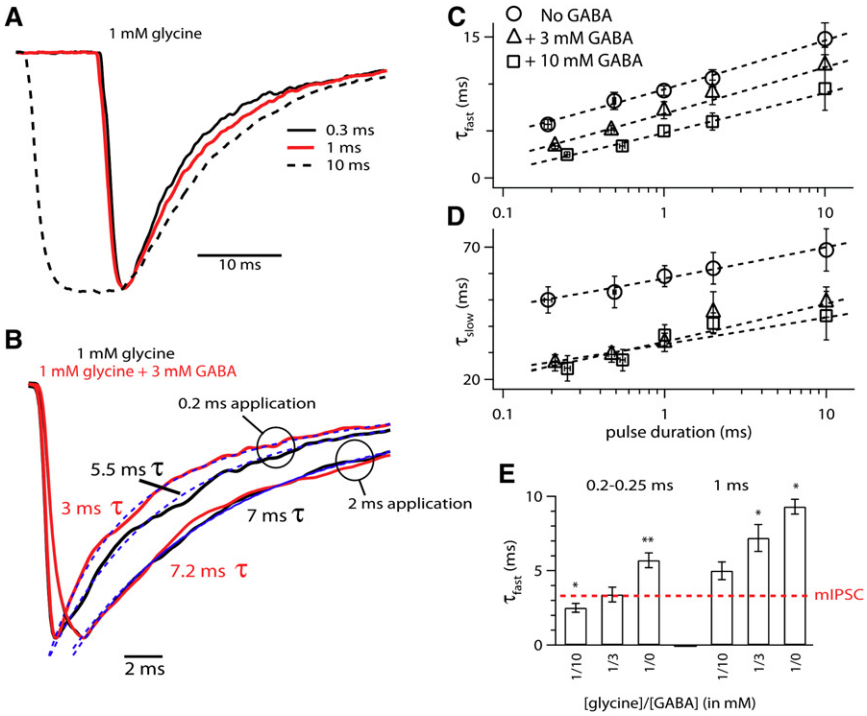

Figure 3. The Decay Kinetics and the Accelerating Effect of GABA Is Sensitive to the Duration of Transmitter Exposure

(A) MNTB patch responses to applications of glycine for various durations (as indicated) were normalized and aligned at the decay. Each trace was the average of 10 to 20 applications.

(B) In another MNTB patch, responses to applications of glycine paired with GABA for various durations (as indicated) were normalized and aligned at the onset. Each trace was the average of 8 to 14 applications. The dashed lines show exponential fits to the decays, with the respective τ_{fast} indicated.

(C and D) Summary of τ_{fast} and τ_{slow} for MNTB patch responses to applications of 1 mM glycine alone (○) or 1 mM glycine paired with 3 mM (△) or 10 mM GABA (□) (n = 11–28 patches for glycine, and n = 4–16 for glycine plus GABA). For each ligand or ligand mix, strong linear correlation was found between the decay times and the logarithm of the application durations ($p < 0.001$).

(E) Comparison of τ_{fast} values shows that, when exposed to a mixture of glycine and GABA very briefly, patches may respond with similar decay kinetics to that of synaptic currents.

Error bars indicate ± SEM.

GABA/glycine-containing and glycine-only boutons at P16, and in terminals containing both transmitters above background, the density of particle labeling was comparable. GABA particles were found at about half the density of glycine in the former population and was similar at P10 and P16 (Figure 5). These data indicate that despite the loss of cotransmission with $GABA_A$ and glycine receptors, GABA is concentrated in the majority of glycine-containing boutons in MNTB.

Regulation of Presynaptic GABA Content

If GABA is coreleased at a majority of synapses and results in a speeding of glycine receptor kinetics, then reduction in presynaptic GABA content should lead to slowing of glycinergic IPSCs. GABA is generated from glutamate by glutamic acid decarboxylase, and block of glutamate uptake into nerve terminals reduces vesicular GABA content (Mathews and Diamond, 2003). We examined the effect of TBOA, a broad-spectrum competitive antagonist of glutamate transporters (Shimamoto et al., 1998), on decay time and amplitude of glycinergic or GABAergic mIPSCs. Baseline values of mIPSC decay time and amplitude were obtained from the recorded cells before 20–30 μM TBOA was bath applied for 15–25 min, followed with wash in TBOA-free perfusate for more than 1 hr. Changes in decay time and amplitude were expressed as percent difference from baseline values, and peak effect was measured by pooling data between the 50th and 70th minute after TBOA application. TBOA increased the decay time of glycinergic mIPSCs (41% ± 3% increase, n = 9, p = 0.0001; Figures 6A, 6B, and 6D). In the absence of TBOA, prolonged whole-cell recordings for up to 2 hr did not change significantly the decay time of glycinergic mIPSCs (8% ± 4% change, n = 6, p = 0.10; Figure 6D). TBOA had only a small effect on the amplitude of glycinergic mIPSCs (15% ± 5% increase, n = 9, p = 0.04; Figure 6A). As expected from previous studies, TBOA reduced the peak amplitude of GABAergic mIPSCs (26% ± 4% reduction, n = 7, p = 0.0006, Figures 6A and 6C), while in the absence of drug, peak amplitude was stable throughout recordings (5% ± 4% change, n = 3, p = 0.34; Figure 6C). TBOA did not alter the decay time of GABAergic mIPSCs (2% ± 4% change, n = 7, p = 0.63; Figure 6A). These effects on glycinergic decays were not due to a direct effect of TBOA on glycine receptors, as the drug did not change the decay time of glycine patch responses (5% ± 9% change, n = 3, p = 0.63). Immediately upon application to the slices (<6 min), TBOA did not significantly affect the kinetics of glycinergic mIPSCs (8% ± 6% change, n = 10, p = 0.22) or the peak amplitude of GABAergic mIPSCs (4% ± 4% change, n = 7, p = 0.36), consistent with the requirement to gradually alter intraterminal transmitter GABA levels. Application of THA, another blocker of glutamate transporters, using the same protocol, also gradually slowed the decay times of glycinergic mIPSCs (21% ± 4% change, n = 6, p = 0.0033; Figure 6D), while reducing the peak amplitude of GABAergic mIPSCs (14% ± 3% decrease, n = 3, p = 0.043; Figure 6C). Another source of presynaptic glutamate is glutamine, which is taken up by the system A transporters and converted to glutamate by glutaminase. Recently it has been shown that blockade of glutamine uptake with the competitive antagonist α-(methylamino) isobutyric acid (MeAIB) (Varoqui et al., 2000) also reduces the GABA content of synapses (Fricke et al., 2007; Liang et al., 2006). Application of MeAIB using the same protocol also produced a marked slowing of the glycine mIPSCs (41% ± 8% increase, n = 6, p = 0.0037; Figure 6D) and a reduction of the amplitude of GABAergic mIPSCs (22% ± 4% reduction, n = 4, p = 0.012; Figure 6C).

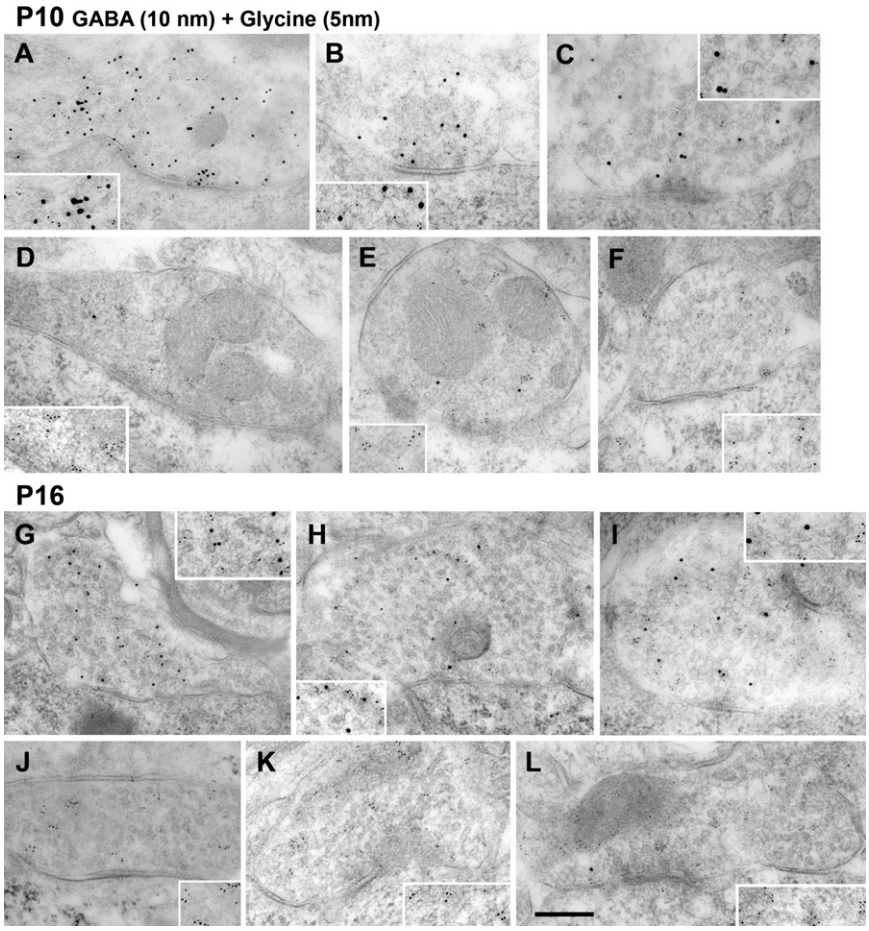

Figure 4. Presynaptic Colocalization of GABA and Glycine

Electron micrographs show postembedding immunogold labeling of GABA and glycine using 10 nm and 5 nm gold particles, respectively, on boutons synapsing on the cell body of MNTB neurons. Top set of six panels (A–F) are from P10 rats, while the lower six panels (G–L) are from P16 rats. In each set, the upper three rows (A–C and G–I) show examples in which both GABA and glycine were found, while the lower three rows (D–F and J–L) show terminals with only glycine labeling. Insets in each case show labeling at higher magnification. Scale bar, 0.2 μm.

This approach to regulation of GABA content was explored further in several ways. Simultaneous application of TBOA and MeAIB for 15–25 min produced an effect similar to that of each drug alone ($p = 0.13$; Figure 6D), possibly because each drug was able to reduce vesicular GABA below a necessary threshold concentration needed to accelerate IPSC kinetics. These data combine recordings from P12–23 rats. When data were divided into 2 week (P12–16) and 3 week (P22–23) age groups, there was no significant difference in the effectiveness of the drugs (56% ± 10% increase, $n = 4$, versus 44% ± 2% increase, $n = 4$, respectively; $p = 0.28$). Thus, it is unlikely that corelease of GABA and glycine is developmentally downregulated in MNTB (see Discussion). We next tested the specificity of these drugs by determining whether their effects on the two transport pathways could be selectively reduced by coapplication of physiological substrates. The effect of TBOA on mIPSC decay could be reduced by coapplication of 2–5 mM glutamate ($p < 0.001$) but not by 4–10 mM glutamine ($p = 0.89$). Conversely, the effect of MeAIB was reduced by glutamine ($p = 0.02$) but not by glutamate ($p = 0.62$) (Figure 6E).

An additional set of slices from P15–17 rats were incubated for 4–8 hr in the GAD inhibitor 3-mercaptopropionic acid (MPA, 250 μM) prior to recordings (Karlsson et al., 1974). The decay time of glycinergic mIPSCs in these slices was 4.4 ± 0.2 ms ($n = 5$), 33% ± 6% slower than that in control slices ($p = 0.005$). Several MPA-incubated slices were bathed in 30 μM TBOA and 4 mM MeAIB for another hour before recordings, and the eventual mIPSC decay time, 4.2 ± 0.1 ms ($n = 6$), was indistinguishable from that with MPA alone ($p = 0.37$). These results are consistent then with the interpretation that TBOA and MeAIB cause a lowering of presynaptic GABA below a critical level needed to impact glycinergic kinetics.

Due to the limited length of recording in single cell (<2 hr), we could not observe the complete time course for the effect of TBOA or MeAIB. Therefore, in a separate series of experiments, 19 slices (P12–17) were incubated for 20–30 min with TBOA (20–30 μM), MeAIB (3–4 mM), or both, then washed for up to 4 hr. When possible, consecutive recordings were made in several cells in the slice throughout the period. Peak effect of TBOA or MeAIB, measured as the decay time of glycinergic mIPSCs pooled from different cells 50–150th min after incubation, revealed a roughly 50% increase over controls (i.e., slices incubated for the same period but without drugs) (Figure 6F); moreover, the glycinergic decay times following the incubation of TBOA (4.7 ± 0.5 ms, $n = 10$, $p = 0.008$ against control), MeAIB (5.0 ± 0.4 ms, $n = 7$, $p = 0.002$), or both (4.5 ± 0.2 ms, $n = 8$, $p = 0.006$) were statistically indistinguishable from one another ($p > 0.26$). Partial recovery was seen in glycinergic mIPSCs recorded after more than 2.5 hr of wash (3.9 ± 0.2 ms, $n = 9$, $p = 0.08$ against control), suggesting GABA may eventually be accumulated in synaptic vesicles at significant concentrations after the interference with glutamate supply is removed. Together these results demonstrate that reduction in presynaptic GABA by two independent transport pathways led to slowing of postsynaptic glycinergic responses.

The Timing of Inhibition

The results described above suggest that cotransmission could shorten the time window for inhibition of EPSPs. To explore the physiological significance for this fine-tuning of synaptic kinetics, we injected MNTB neurons at physiological temperature with excitatory and inhibitory synaptic-like inputs using

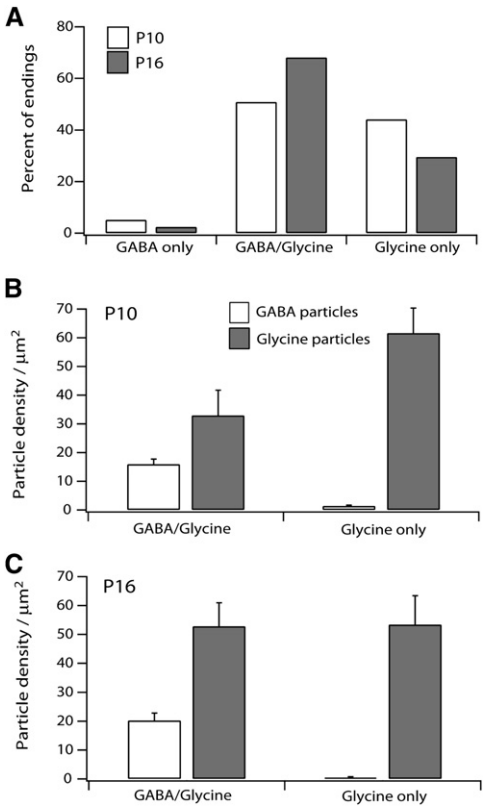

Figure 5. GABA Is Present in the Majority of Glycinergic Boutons in MNTB

(A) Histogram shows the percent of endings analyzed that were found labeled for only GABA, only glycine, or colabeled with GABA and glycine (GABA/Glycine) for P10 and P16 rats. At both ages, the GABA/Glycine endings were most highly represented. N = 103 boutons (P10 = 59, P16 = 44) on cell bodies of MNTB neurons.

(B and C) Density of gold particles per area of synaptic ending ± SEM in P10 and P16 rats, respectively. By P16, the density of glycine labeling was similar in glycine-only and GABA/glycine-containing boutons.

a two-electrode conductance-clamp configuration (Figure 7A). The strength of the excitatory postsynaptic conductance (EPSG) was fixed either at threshold (18 ± 3.5 nS, spiking probability = 0.5 ± 0.1, n = 5) or 10∼30% above threshold (spiking probability = 1.0) in the absence of inhibition. Only the time delay by which the inhibitory postsynaptic conductance (IPSG) led EPSG was varied systematically, from 0 to 15 ms; in practice, the action potential was completely blocked when the IPSG led EPSG by only a few milliseconds. With the parameter set used in Figure 7B, reducing the IPSG decay constant from 2 ms to 1 ms resulted in halving the maximal interval between IPSG and EPSG that resulted in spike blockade.

We quantified this temporal precision needed for effective inhibition with an "inhibition window," defined as the maximum lead time that still allowed the IPSG to block all action potentials induced by EPSG. With suprathreshold EPSG, the lengthening in IPSG decay time constant resulted in a nearly proportional expansion of the inhibition window (2.4 ± 0.2 ms for τ_{decay} = 1 ms, 4.1 ± 0.4 ms for τ_{decay} = 2 ms, n = 5; Figure 7C, circles). Inhibition window grew even more steeply for at-threshold EPSGs (3.6 ± 0.2 ms for τ_{decay} = 1 ms, 7.7 ± 0.5 ms for τ_{decay} = 2 ms, n = 5; Figure 7C, squares) and were always longer for threshold EPSGs than for suprathreshold EPSGs (Figure 7C, squares versus circles, $p < 0.01$). Our data indicate that, depending on the strength of excitatory input, a small change in the decay time constant for inhibitory conductance may affect postsynaptic activity for periods several times longer. This observation depends critically on the relative strengths of EPSG and IPSG—an EPSG several times stronger than the IPSG would render the IPSG less effective or the inhibition window less sensitive to changes in IPSG kinetics. However, given that the excitatory input may be chronically depressed to near-threshold levels in vivo (Hermann et al., 2007) and that IPSCs in MNTB do not depress as readily (Awatramani et al., 2004), regulation of the IPSC decay time would be likely to impact the effective coincidence time of inhibitory and excitatory signals.

DISCUSSION

Cotransmission Regulates Glycinergic Signals

Colocalization and release of GABA and glycine is widespread in inhibitory neurons of the brainstem and spinal cord. We show for the first time that GABA, coreleased with glycine from the same vesicles, acts as a coagonist to modify the response of glycine receptors to glycine. In the MNTB, and elsewhere in the auditory pathway where rapid phasic signaling is required for processing of acoustic information, this novel form of cotransmission appears to be well suited to refining the kinetics of inhibition. The MNTB transmits inhibitory signals to nuclei of the superior olive with delays, in cats, of less than 200 µs (Joris and Yin, 1998), emphasizing the importance of structural and physiological adaptations in the MNTB to reducing synaptic and conduction delays (Taschenberger et al., 2002). This rapid inhibition is utilized in encoding interaural intensity, and possibly also timing differences, in the lateral and medial superior olives (LSO and MSO), respectively (Brand et al., 2002; Tollin, 2003). MNTB neurons best activated by a given frequency of sound can be inhibited by sounds of higher or lower frequencies (Kopp-Scheinpflug et al., 2003); such glycinergic inhibition is triggered and terminated rapidly with the onset and offset of the sideband stimuli. The kinetics of glycinergic signals would impact how quickly such acoustic inhibition could act during complex, behaviorally relevant sounds. Corelease of GABA and glycine, combined with short transmitter lifetimes, allow inhibition to sculpt precisely the response pattern of the MNTB.

Colocalization of GABA and glycine are characteristic of neonatal brain, and shifts from cotransmission to glycine-only transmission have been documented in several brain regions (Awatramani et al., 2005; Kotak et al., 1998; Muller et al., 2006; Nabekura et al., 2004). In some cases, loss of presynaptic GABA may underlie this shift (Muller et al., 2006; Nabekura et al., 2004). Our results indicate that, in other cases, GABA release may be retained by older animals, even when IPSCs are no longer mediated by $GABA_A$ receptors. GABA and glycine were found in the majority of MNTB terminals in P16 rats, when GABA was reported missing in LSO and motoneurons (Muller et al., 2006; Nabekura et al., 2004). In P16 rats, the GABA labeling was absent in about

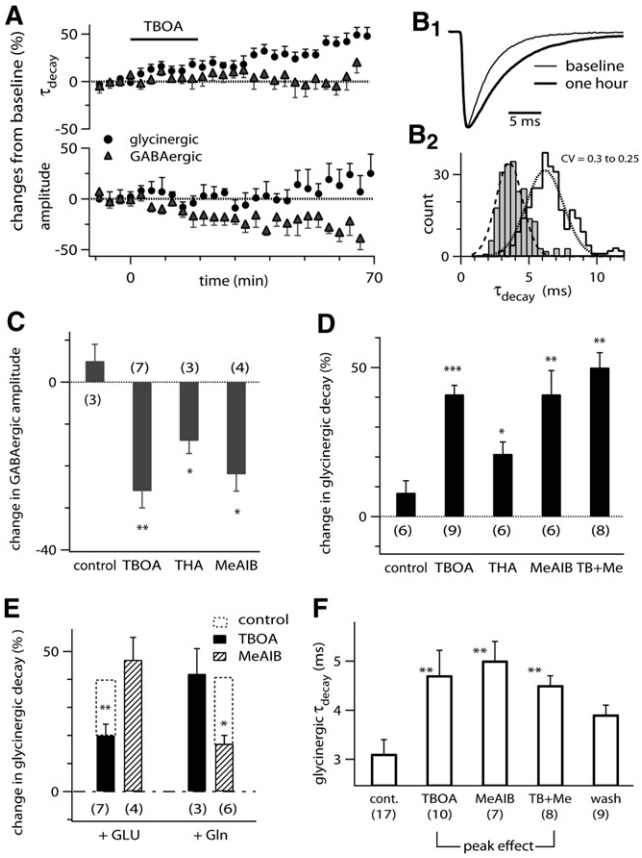

Figure 6. Reduction in Intraterminal GABA Concentration Slows the Decay of Glycinergic Synaptic Responses

(A) The running average (every 3 min) of the decay times and peak amplitude of glycinergic (●) or GABAergic mIPSC (▲), normalized to baseline values. Glycinergic mIPSCs (n = 9 cells, rats aged P10–19) and GABAergic mIPSCs (n = 7 cells, rats aged P10–15) were both pharmacologically isolated. Metabotropic glutamate receptors and $GABA_B$ receptors were blocked with a cocktail of antagonists including 20 μM LY-341495, 30 μM E4CPG, 30 μM CPPG, and 2 μM CGP-54828.

(B_1) Normalized glycinergic mIPSCs, averaged over the baseline period or over the 50–70th min following TBOA application in one cell (P18). (B_2) Distributions of the decay time constant for glycinergic mIPSCs over these same periods from same cell. Both distributions for the baseline (lightly shaded) and after-TBOA (hollow envelope) events were best fitted with a Gaussian distribution (dashed line).

(C) The effect of TBOA (20–30 μM), THA (300 μM), and MeAIB (4 mM) on intraterminal GABA concentration, measured by baseline-normalized peak amplitude of GABAergic mIPSC about 1 hr following a 15–25 min bath application of each blocker. In control experiments where blockers were not added, prolonged recordings for up to 1.5 hr revealed no significant change. Numbers in parentheses indicate number of cells; statistical significance was tested against the baseline.

(D) Baseline-normalized decay times for glycinergic mIPSCs in a similar series of experiments. The increases mirrored the reductions in amplitude of GABAergic mIPSCs. Control recordings in the absence of blockers showed that decay kinetics were stable for up to 2 hr.

(E) Effect of TBOA on the decay time of glycinergic mIPSCs was significantly reduced with coapplication of glutamate (2–5 mM), but not glutamine (4–10 mM). Conversely, the effect of MeAIB was reduced only with the coapplication of glutamine. Note statistical significance was tested against the effects of TBOA or MeAIB alone.

one-third of the glycine-labeled boutons, where the intraterminal GABA level might have been too low for the antibody to pick up. Nevertheless, these boutons may still corelease some GABA, because the vesicular transporter has a higher affinity for GABA than for glycine, and the vesicles accumulate GABA twice as fast (Christensen and Fonnum, 1991; McIntire et al., 1997). Our data do not support that a significant portion of glycinergic synapses in MNTB are distinct in not coreleasing GABA at all, because the mIPSC decay times were best described with a Gaussian distribution (Figure 6B_2). Moreover, no difference was seen in the ability of glutamate uptake blockers to prolong IPSCs between ages P10 to P23. On the other hand, the significant reduction in coefficient of variation for these decay times from baseline to 1 hr following TBOA application (0.35 ± 0.04 versus 0.27 ± 0.03, n = 9, p = 0.013) suggested an intersynaptic variability in GABA content that could be reduced with interference in GABA synthesis. Given the persistence of coexpression of these two transmitters in a subset of adult glycinergic neurons in other species as well, including baboon, bat, cat, guinea pig, and rat (Alibardi, 2003; Kemmer and Vater, 1997; Kolston et al., 1992; Moore et al., 1996; Osen et al., 1990; Ostapoff et al., 1997; Rubio and Juiz, 2004; Saint Marie et al., 1991, 1997; Wenthold and Hunter, 1990), it seems likely that cotransmission is a general means for fine-tuning glycinergic transmission in the mature auditory system.

Such a role for modulated inhibition stands in sharp contrast to purely GABAergic signaling within the auditory brainstem. IPSCs mediated by $GABA_A$ receptors not only provide stable inhibition during acoustic stimuli, but also sharply reduce excitability for tens of milliseconds after a stimulus (Klug et al., 1999; Kulesza et al., 2007; Pecka et al., 2007). This is a result both of the slower $GABA_A$ receptor deactivation after each stimulus, but also enhanced asynchronous quantal release (Lu and Trussell, 2000; Pecka et al., 2007). It is interesting in this regard that even within the MNTB, transmission mediated by $GABA_A$ and glycine receptors differ significantly in both decay times and the time course of quantal release (Awatramani et al., 2005). These results highlight that GABA may be used for very distinct purposes characterized by different time courses, depending on whether it targets $GABA_B$, $GABA_A$, or glycine receptors.

Other roles for cotransmission by GABA and glycine have been proposed. Where both ionotropic receptors are present, GABA and glycine produce IPSCs with a distinct multiphasic time course (Awatramani et al., 2005; Jonas et al., 1998; Russier et al., 2002). Terminals of cerebellar Golgi cells corelease both transmitters, but their postsynaptic effects vary with the target: granule cells only sense GABA, and unipolar brush cells only sense glycine (Dugué et al., 2005). In spinal dorsal horn neurons, coreleased GABA acts on extrasynaptic $GABA_A$ receptors only during intense activation (Chéry and de Koninck, 2000).

(F) In separate experiments, 19 slices were incubated for 20–30 min with TBOA (20–30 μM), MeAIB (3–4 mM), or both, then washed for up to 4 hr in perfusate containing the same mGluR and $GABA_B$ blockers as above. "Peak effect" was obtained from events pooled during the 50–150 min after incubation. Partial recovery in glycinergic decay time was seen in recordings made after 2.5 hr of wash (data pooled from all three conditions).

Error bars indicate ± SEM.

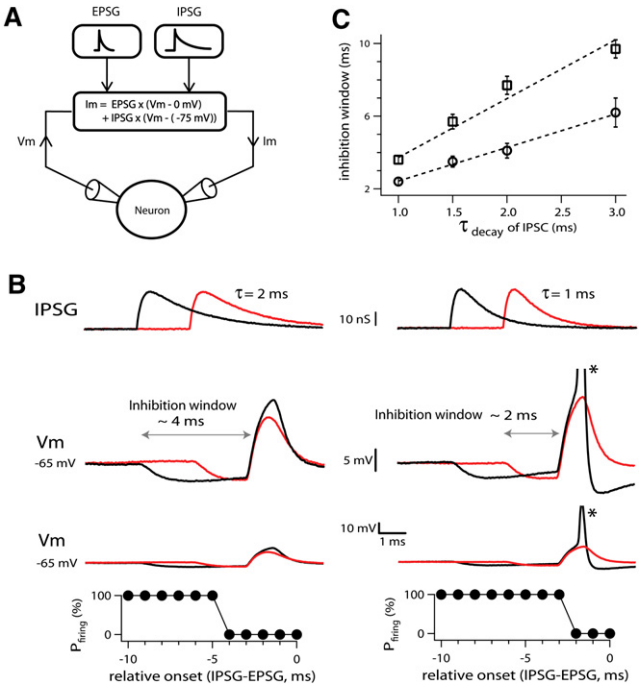

Figure 7. Inhibition Window of Inhibitory Conductance Was Highly Sensitive to Changes in Decay Kinetics

(A) Schematic of two-electrode conductance-clamp strategy.

(B) Top lines show timing and durations of IPSGs. Lower lines are voltage traces shown at two gain settings, all from a single cell. The EPSG had a peak value of 21 nS and produced a spiking probability of 100% in the absence of IPSG. The IPSG had a constant peak magnitude of 25 nS, and was delivered in this example either 2 or 4 ms before EPSG. Action potential is marked with an asterisk. Lower plots show firing probability versus relative timing of IPSG-EPSG onsets for this cell.

(C) Inhibition window, defined as the maximum lead time the IPSG had before the EPSG and still block all action potentials. This window expands proportionally to the decay time constant of IPSGs. Linear fit to the data had a slope of 1.9 for suprathreshold EPSG (circles), 3.0 for threshold EPSG (squares), and a correlation coefficient >0.98 for both (n = 5 neurons).

Error bars indicate ± SEM.

Coreleased GABA may also act presynaptically to inhibit GABA and glycine release in spinal cord and cochlear nucleus (Chéry and de Koninck, 1999; Lim et al., 2000). Our results indicate that, apart from any secondary action of GABA outside the synaptic cleft, the two transmitters may work together at a single receptor to enhance the temporal resolution of inhibition.

Recent studies suggest that presynaptic glutamate pools maintained by plasma membrane transporters support GABAergic transmission. Our study indicates that these pools may also play a role in GABA/glycine cotransmission. Several differences were observed with some previous work. We found that effects of transport blockers arose only after a long delay and recovered incompletely. Given that our study focused on measurements of mIPSCs rather than evoked events, this delay may reflect the slow turnover of vesicle populations in unstimulated synapses or the gradual depletion of endogenous GABA levels. Recovery of GABA-filled vesicles may reflect differences in refilling rates for GABA versus glycine (Katsurabayashi et al., 2004). Liang et al. (2006) observed an effect of MeAIB only on IPSCs following high-frequency synaptic activity and could not occlude this action with exogenous glutamine. Other groups have observed acute and reversible effects of MeAIB on mIPSCs or low-frequency evoked IPSCs (Chaudhry et al., 2002; Fricke et al., 2007). By contrast, we observed an effect of MeAIB on mIPSCs after a long delay and found competition of the effect by glutamine, as expected for transported substrates (Varoqui et al., 2000). It is possible that glutamine and MeAIB could reversibly alter release by depolarizing synapses (Chaudhry et al., 2002; Kam and Nicoll, 2007). This confound could not account for our results, since we only measured mIPSCs after MeAIB washout.

Exposure Dependence of Current Decays

Glycine receptors deactivated more slowly following longer applications of glycine. This effect was previously noted by Mohammadi et al. (2003) for longer-duration pulses on glycine receptors and may be relatively common to synaptic receptors. For example, Zhang et al. (2006) observed this effect in heterologously expressed AMPA receptors, ascribing it to progressive occupancy of more openable states as more agonist molecules bind. Jones and Westbrook (1995) found a similar effect for GABA receptors and argued that longer GABA exposure leads to slower deactivation as desensitized receptors transiently reopen before unbinding. Regardless of the kinetic mechanism, this effect may have significant impact on synaptic transmission, since the time course of transmitter might vary with subtle variation in synaptic morphology or density and distribution of transporters (Cathala et al., 2005; Renden et al., 2005).

Mechanism of Glycine-GABA Interactions

Our results show that GABA acted directly on the glycine-binding subunit of the glycine receptor. Previous studies indicated that GABA is a weak partial agonist of the receptor, producing smaller currents with a much higher EC_{50} of tens of millimolar (De Saint Jan et al., 2001; Jonas et al., 1998; Lewis et al., 2003). Moreover, gabazine, an effective antagonist of $GABA_A$ receptors, is a low-affinity antagonist of glycine receptors (Beato et al., 2007), further emphasizing that glycine binding sites have limited selectivity for ligands characteristic of both glycine and $GABA_A$ receptors. Glycine receptors require occupation of two to three sites for full activation, although channel opening by fewer ligands might occur (Burzomato et al., 2004), producing open states of shorter duration. Consistent with competition at these binding sites, the effect of GABA on peak amplitude and decay kinetics increased with the GABA/glycine ratio. Two scenarios might account for the more rapid kinetics we see when glycine receptors are exposed to both GABA and glycine. First, the occupation of a fraction of the binding sites by GABA might simply displace glycine molecules and induce channel openings characteristic of a partially glycine-bound receptor. This possibility cannot fully account for our observations, since applications of glycine concentrations between 0.3 and 10 mM did not exhibit differences in current deactivation time (Figure S1C), and concentrations lower than these would give open probabilities too low to be consistent with estimated values at synapses (Jonas et al., 1998; Rigo et al., 2003; Singer and Berger, 1999;

Suwa et al., 2001). A stronger alternative is based on the concept that channel gating properties (e.g., stability of the active, open state) depend upon the identity of the bound ligand (Colquhoun and Sakmann, 1985; Del Castillo and Katz, 1957). Indeed, glycine receptors activated by very high concentrations of GABA have deactivation times ten times faster than receptors activated by glycine (Fucile et al., 1999). We propose the stability of the channel open state of receptors (and thus the deactivation time) with both GABA and glycine bound is intermediate between the glycine-bound or GABA-bound receptors. Because this effect of GABA is characteristic of the major glycine-binding subunit in the brain, we suggest that its coagonist role in transmission may be common to all glycinergic synapses where colocalization is found. Our results provide a novel mechanism by which postsynaptic responses may be modulated. Other modulators of synaptic kinetics may either operate at the level of the entire cell, changing its membrane time constant, or alter the structure of the postsynaptic receptor, subunit composition, or phosphorylation state. Our results suggest that by combining weak or partial agonists with full agonists in single vesicles, synapses may take advantage of the wide range of affinities of different endogenous compounds for receptor sites in order to fine-tune the duration of the postsynaptic response. In principle, such a mechanism has the advantage of tuning the magnitude and duration of a synapse-specific postsynaptic effect by grading the relative concentrations of transmitters.

EXPERIMENTAL PROCEDURES

Preparations and Solutions

The handling and care of animals was approved by the OHSU and University of Connecticut Institutional Animal Care & Use Committees. Brainstem slices (200 μm) were prepared from P10–23 Wistar rats in low-Ca^{2+}, low-Na^{+} saline (Awatramani et al., 2004, 2005) and incubated in 30°C ACSF for 1 hr before recording. The ACSF for incubation and recording contained (in mM) 125 NaCl, 25 $NaHCO_3$, 5 KCl, 2 $CaCl_2$, 1 $MgCl_2$, 1 NaH_2PO_4, 0.4 L-ascorbic acid, 3 myo-inositol, 2 Na-pyruvate, and 25 glucose (pH 7.4, saturated with 95% O_2/5% CO_2). NaCl and HEPES replaced $NaHCO_3$ for the ACSF used on outside-out patches. The protocol for isolating MNTB neurons were adapted from that used previously (Raman et al., 1994). The recording pipettes were filled with (in mM) 130 CsCl, 10 TEA.Cl, 2 $MgCl_2$, 10 HEPES, 5 BAPTA.Cs_4, 4 QX-314.Cl, and 2–4 Mg.ATP (pH 7.2 with CsOH). Glutamate or GABA receptor antagonists (50 μM APV, 20 μM DNQX, 20 μM SR-95531) and 1 μM tetrodotoxin were included in the ACSF when recording glycinergic miniature IPSCs. Strychnine (0.5–1 μM) was substituted for SR-95531 when recording GABAergic miniature IPSCs. All synaptic activity was blocked in the presence of glutamate-, GABA-, and glycine-receptor antagonists. Reagents were from Sigma-Aldrich, Tocris, and Alamone.

Homomeric Receptor Expression

Human embryonic kidney 293 cells (HEK293) (American Type Culture Collection-CRL-1573) were maintained at 37°C in a 95% air/5% CO_2 incubator in DMEM supplemented with 0.11 g/l sodium pyruvate, 10% v/v heat-inactivated fetal bovine serum, 100 U/ml penicillin G, 100 μg/ml streptomycin sulfate, and 2 mM L-glutamine and passaged every 2–3 days, up to 20 times. Cells were plated on coverslips, to reach a moderate density, and then transfected by Lipofectamin reagent with cDNAs for the human α1 receptor subunit, a gift of Dr. J. Mihic, UT Austin. cDNA for enhanced green fluorescent protein plasmid (EGFP-c1) was cotransfected with 3 μg of receptor cDNA to allow detection of transfected cells. Patch-clamp recordings were made 14–48 hr after transfection.

Recordings

Whole-cell and outside-out patch recordings were made at room temperature. Recording pipettes pulled from borosilicate glass typically had a resistance of 3–5 MΩ, and in whole-cell recordings the series resistance was compensated by 80% using an Axopatch 200B amplifier (Molecular Devices). Holding potential was –60 mV.

Drug Application

The fabrication of theta-pipettes and set-up of piezo-driven fast-flow system was as previously described (Raman et al., 1994). The 20%–80% solution exchange time, measured by the instant change in open-tip junction potential between the normal and a 10%-diluted ACSF, was typically 30–80 μs. Two three-way manifolds were installed close to the back of the theta-pipette, and consequently both the control and test solutions could be completely changed within 20 s. Control experiments were conducted to estimate the solution exchange time over intact patches and whether effective agonist concentration at receptors is reduced for very brief applications (see Figure S4 and associated text). This was accomplished by applying 1 mM kainic acid to patches and measuring the change in current upon rapid exchange of Na^{+} concentration from 40 to 140 mM. The results showed that the rise time of such responses were slightly slower than with junction potential measurements on the same electrodes (130 μs versus 76 μs). For our shortest applications (0.2–0.25 ms), the reduction in agonist concentration was 13%–17% and was essentially full-amplitude for longer applications (Figure S4).

Conductance Clamp

Two-electrode whole-cell recordings were made from P15–18 neurons at 35°C–37°C; the membrane potential was monitored through one electrode, whereas the simulated synaptic currents from a conductance clamp circuit (SM-1, Cambridge Conductance, Cambridge, UK) were injected through the other. This configuration eliminated the error in membrane potential resulting from the large injection currents passing across the electrode series resistance. Electrode internal solution contained (in mM) 147 K-gluconate, 5 KCl, 1 $MgCl_2$,10 HEPES, 4 BAPTA, 4 Mg-ATP, pH 7.2, with correction for a 12 mV junction potential. EPSGs were generated by the sum of two exponentials with τ_{rise} = 0.1 ms, τ_{decay} = 0.4 ms, and set to reverse at 0 mV; IPSGs were generated by the sum of two exponentials with τ_{rise} = 0.2 ms, τ_{decay} = 1∼3 ms, and set to reverse at –75 mV (Awatramani et al., 2004, 2005). The peak IPSG was set to 20∼30 nS, based on reported amplitude of single-axon evoked IPSCs (Awatramani et al., 2005). After first determining threshold excitatory conductance needed to trigger 50% firing probability, we set the peak EPSG to threshold or 10%–30% above threshold. The IPSG was delivered at 0–15 ms (at intervals ≤1 ms, in random order) before the EPSG. The EPSG-IPSG pairing was repeated 100 times at 2–10 Hz.

Electron Microscopy

A total of two P10 and two P16 Sprague-Dawley rats were used in these experiments. A mixture of ketamine (60 mg/kg body weight) and xylazine (6.5 mg/kg body weight) was injected intramuscularly to induce deep anesthesia before transcardial perfusion with 4% paraformaldehyde and 0.5% glutaraldehyde in 0.12 M phosphate buffer, pH 7.2. Brains were removed, fixed for an hour at 4°C, rinsed in buffer, and stored overnight at 4°C. Brainstems were sliced on a vibratome and the slices processed for freeze-substitution technique followed by postembedding immunogold labeling (see below). The MNTB was trimmed from 300 μm thick brainstem sections and processed for freeze-substitution and low-temperature embedding as previously described (Rubio, 2006; Rubio and Wenthold, 1997). Double postembedding immunogold labeling for GABA and glycine (1:400 each; Chemicon, Temecula) was performed as previously described (Rubio, 2006). Primary antibodies were labeled with 5 nm (Glycine) or 10 nm (GABA) colloidal gold-coupled secondary antibodies (Amersham, Piscataway). Controls were carried out by omitting the primary antibody in the immunogold labeling. Immunostaining was analyzed with a TECNAI 12 Biotwin TEM. The images were captured with an AMT CCD camera at 49,000× magnification. Image processing was performed with Adobe Photoshop by using only the brightness and contrast commands to enhance gold particles. The quantitative analysis of GABA and glycine on synaptic endings on cell bodies of MNTB neurons was analyzed in a total of 103 endings

(P10 n = 59 and P16 n = 44). The density of gold particles for GABA and/or glycine was computed using JScion NIH image for each synaptic ending profile by dividing the number of gold particles in a synaptic ending profile by the cytoplasmic area of that profile. The average density was computed across all profiles. The synaptic ending were classified as GABAergic if they were only immunogold labeled for GABA, glycinergic for only glycine, and GABA/Gly when they were double labeled for GABA and glycine. The three categories of synaptic endings contained flattened and/or pleomorphic synaptic vesicles and made Gray Type II symmetric synapses on the cell bodies of MNTB neurons; some of these endings were also observed on dendrites. Gold particles on mitochondria or on putative excitatory synapses containing rounded synaptic vesicles were low and were considered background, and their density subtracted from that measured at inhibitory terminals. A bouton was considered labeled if it contained more than four particles; the background levels for either glycine or GABA was therefore a maximum of three particles, and the majority of unlabeled structures had between zero or two particles.

Data Analyses and Statistics

The current responses were acquired in pClamp 9 (Molecular Devices) and analyzed with Axograph 4.9 (Molecular Devices) and Igor 5.0 (Wavemetrics). Unless specified otherwise, summary data were presented as mean ± SEM, and statistical significance was established using t tests as appropriate.

SUPPLEMENTAL DATA

The Supplemental Data for this article can be found online at http://www.neuron.org/cgi/content/full/57/4/524/DC1/.

ACKNOWLEDGMENTS

We thank Drs. Gail Mandel, Trillium Blackmer, and Hai Huang for critical comments; and Dr. Viktor Derkach for assistance with transfections. Supported by NIH grants DC04455 to L.O.T and DC006881-01A2 to M.E.R. NSF DBI-0420580 contributed funds to purchase the Tecnai 12 Biotwin.

Received: May 16, 2007
Revised: November 26, 2007
Accepted: December 6, 2007
Published: February 27, 2008

REFERENCES

Alibardi, L. (2003). Ultrastructural distribution of glycinergic and GABAergic neurons and axon terminals in the rat dorsal cochlear nucleus, with emphasis on granule cell areas. J. Anat. *203*, 31–56.

Awatramani, G.B., Turecek, R., and Trussell, L.O. (2004). Inhibitory control at a synaptic relay. J. Neurosci. *24*, 2643–2647.

Awatramani, G.B., Turecek, R., and Trussell, L.O. (2005). Staggered development of GABAergic and glycinergic transmission in the MNTB. J. Neurophysiol. *93*, 819–828.

Beato, M., Burzomato, V., and Sivilotti, L.G. (2007). The kinetics of inhibition of rat recombinant heteromeric alpha1beta glycine receptors by the low-affinity antagonist SR-95531. J. Physiol. *580*, 171–179.

Brand, A., Behrend, O., Marquardt, T., McAlpine, D., and Grothe, B. (2002). Precise inhibition is essential for microsecond interaural time difference coding. Nature *417*, 543–547.

Burzomato, V., Beato, M., Groot-Kormelink, P.J., Colquhoun, D., and Sivilotti, L.G. (2004). Single-channel behavior of heteromeric alpha1beta glycine receptors: an attempt to detect a conformational change before the channel opens. J. Neurosci. *24*, 10924–10940.

Cathala, L., Holderith, N.B., Nusser, Z., DiGregorio, D.A., and Cull-Candy, S.G. (2005). Changes in synaptic structure underlie the developmental speeding of AMPA receptor-mediated EPSCs. Nat. Neurosci. *8*, 1310–1318.

Chaudhry, F.A., Reimer, R.J., Bellocchio, E.E., Danbolt, N.C., Osen, K.K., Edwards, R.H., and Storm-Mathisen, J. (1998). The vesicular GABA transporter, VGAT, localizes to synaptic vesicles in sets of glycinergic as well as GABAergic neurons. J. Neurosci. *18*, 9733–9750.

Chaudhry, F.A., Schmitz, D., Reimer, R.J., Larsson, P., Gray, A.T., Nicoll, R., Kavanaugh, M., and Edwards, R.H. (2002). Glutamine uptake by neurons: interaction of protons with system a transporters. J. Neurosci. *22*, 62–72.

Chéry, N., and de Koninck, Y. (1999). Junctional versus extrajunctional glycine and GABA(A) receptor-mediated IPSCs in identified lamina I neurons of the adult rat spinal cord. J. Neurosci. *19*, 7342–7355.

Chéry, N., and de Koninck, Y. (2000). GABA(B) receptors are the first target of released GABA at lamina I inhibitory synapses in the adult rat spinal cord. J. Neurophysiol. *84*, 1006–1011.

Christensen, H., and Fonnum, F. (1991). Uptake of glycine, GABA and glutamate by synaptic vesicles isolated from different regions of rat CNS. Neurosci. Lett. *129*, 217–220.

Clements, J.D., Lester, R.A., Tong, G., Jahr, C.E., and Westbrook, G.L. (1992). The time course of glutamate in the synaptic cleft. Science *258*, 1498–1501.

Colquhoun, D., and Sakmann, B. (1985). Fast events in single-channel currents activated by acetylcholine and its analogues at the frog muscle end-plate. J. Physiol. *369*, 501–557.

De Saint Jan, D., David-Watine, B., Korn, H., and Bregestovski, P. (2001). Activation of human alpha1 and alpha2 homomeric glycine receptors by taurine and GABA. J. Physiol. *535*, 741–755.

Del Castillo, J., and Katz, B. (1957). Interaction at end-plate receptors between different choline derivatives. Proc. R. Soc. Lond. B. Biol. Sci. *146*, 369–381.

Dugué, G.P., Dumoulin, A., Triller, A., and Dieudonné, S. (2005). Target-dependent use of co-released inhibitory transmitters at central synapses. J. Neurosci. *25*, 6490–6498.

Friauf, E., Hammerschmidt, B., and Kirsch, J. (1997). Development of adult-type inhibitory glycine receptors in the central auditory system of rats. J. Comp. Neurol. *385*, 117–134.

Fricke, M.N., Jones-Davis, D.M., and Mathews, G.C. (2007). Glutamine uptake by System A transporters maintains neurotransmitter GABA synthesis and inhibitory synaptic transmission. J. Neurochem. *102*, 1895–1904.

Fucile, S., de Saint Jan, D., David-Watine, B., Korn, H., and Bregestovski, P. (1999). Comparison of glycine and GABA actions on the zebrafish homomeric glycine receptor. J. Physiol. *517*, 369–383.

Gleich, O., and Vater, M. (1998). Postnatal development of GABA- and glycine-like immunoreactivity in the cochlear nucleus of the Mongolian gerbil (Meriones unguiculatus). Cell Tissue Res. *293*, 207–225.

Harty, T.P., and Manis, P.B. (1998). Kinetic analysis of glycine receptor currents in ventral cochlear nucleus. J. Neurophys. *79*, 1891–1901.

Hermann, J., Pecka, M., von Gersdorff, H., Grothe, B., and Klug, A. (2007). Synaptic transmission at the calyx of Held under in vivo like activity levels. J. Neurophysiol. *98*, 807–820.

Jonas, P., Bischofberger, J., and Sandkuhler, J. (1998). Corelease of two fast neurotransmitters at a central synapse. Science *281*, 419–424.

Jones, M.V., and Westbrook, G.L. (1995). Desensitized states prolong GABAA channel responses to brief agonist pulses. Neuron *15*, 181–191.

Joris, P.X., and Yin, T.C. (1998). Envelope coding in the lateral superior olive. III. Comparison with afferent pathways. J. Neurophysiol. *79*, 253–269.

Kam, K., and Nicoll, R. (2007). Excitatory synaptic transmission persists independently of the glutamate-glutamine cycle. J. Neurosci. *27*, 9192–9200.

Karlsson, A., Fonnum, F., Malthe-Sorenssen, D., and Storm-Mathisen, J. (1974). Effect of the convulsive agent 3-mercaptopropionic acid on the levels of GABA, other amino acids and glutamate decarboxylase in different regions of the rat brain. Biochem. Pharmacol. *23*, 3053–3061.

Katsurabayashi, S., Kubota, H., Higashi, H., Akaike, N., and Ito, Y. (2004). Distinct profiles of refilling of inhibitory neurotransmitters into presynaptic terminals projecting to spinal neurones in immature rats. J. Physiol. *560*, 469–478.

Kemmer, M., and Vater, M. (1997). The distribution of GABA and glycine immunostaining in the cochlear nucleus of the mustached bat (Pteronotus parnellii). Cell Tissue Res. *287*, 487–506.

Klug, A., Bauer, E.E., and Pollak, G.D. (1999). Multiple components of ipsilaterally evoked inhibition in the inferior colliculus. J. Neurophysiol. *82*, 593–610.

Kolston, J., Osen, K.K., Hackney, C.M., Ottersen, O.P., and Storm-Mathisen, J. (1992). An atlas of glycine- and GABA-like immunoreactivity and colocalization in the cochlear nuclear complex of the guinea pig. Anat. Embryol. (Berl.) *186*, 443–465.

Kopp-Scheinpflug, C., Lippe, W.R., Dorrscheidt, G.J., and Rubsamen, R. (2003). The medial nucleus of the trapezoid body in the gerbil is more than a relay: comparison of pre- and postsynaptic activity. J. Assoc. Res. Otolaryngol. *4*, 1–23.

Korada, S., and Schwartz, I.R. (1999). Development of GABA, glycine, and their receptors in the auditory brainstem of gerbil: a light and electron microscopic study. J. Comp. Neurol. *409*, 664–681.

Kotak, V.C., Korada, S., Schwartz, I.R., and Sanes, D.H. (1998). A developmental shift from GABAergic to glycinergic transmission in the central auditory system. J. Neurosci. *18*, 4646–4655.

Kulesza, R.J., Jr., Kadner, A., and Berrebi, A.S. (2007). Distinct roles for glycine and GABA in shaping the response properties of neurons in the superior paraolivary nucleus of the rat. J. Neurophysiol. *97*, 1610–1620.

Leao, R.N., Oleskevich, S., Sun, H., Bautista, M., Fyffe, R.E., and Walmsley, B. (2004). Differences in glycinergic mIPSCs in the auditory brain stem of normal and congenitally deaf neonatal mice. J. Neurophysiol. *91*, 1006–1012.

Lewis, T.M., Schofield, P.R., and McClellan, A.M. (2003). Kinetic determinants of agonist action at the recombinant human glycine receptor. J. Physiol. *549*, 361–374.

Liang, S.L., Carlson, G.C., and Coulter, D.A. (2006). Dynamic regulation of synaptic GABA release by the glutamate-glutamine cycle in hippocampal area CA1. J. Neurosci. *26*, 8537–8548.

Lim, R., Alvarez, F.J., and Walmsley, B. (2000). GABA mediates presynaptic inhibition at glycinergic synapses in a rat auditory brainstem nucleus. J. Physiol. *525*, 447–459.

Lu, T., and Trussell, L.O. (2000). Inhibitory transmission mediated by asynchronous transmitter release. Neuron *26*, 683–694.

Magnusson, A.K., Kapfer, C., Grothe, B., and Koch, U. (2005). Maturation of glycinergic inhibition in the gerbil medial superior olive after hearing onset. J. Physiol. *568*, 497–512.

Mathews, G.C., and Diamond, J.S. (2003). Neuronal glutamate uptake contributes to GABA synthesis and inhibitory synaptic strength. J. Neurosci. *23*, 2040–2048.

McIntire, S.L., Reimer, R.J., Schuske, K., Edwards, R.H., and Jorgensen, E.M. (1997). Identification and chacterization of the vesicular GABA transporter. Nature *389*, 870–876.

Mohammadi, B., Krampfl, K., Cetinkaya, C., Moschref, H., Grosskreutz, J., Dengler, R., and Bufler, J. (2003). Kinetic analysis of recombinant mammalian alpha(1) and alpha(1)beta glycine receptor channels. Eur. Biophys. J. *32*, 529–536.

Moore, J.K., Osen, K.K., Storm-Mathisen, J., and Ottersen, O.P. (1996). gamma-Aminobutyric acid and glycine in the baboon cochlear nuclei: an immunocytochemical colocalization study with reference to interspecies differences in inhibitory systems. J. Comp. Neurol. *369*, 497–519.

Muller, E., Le Corronc, H., Triller, A., and Legendre, P. (2006). Developmental dissociation of presynaptic inhibitory neurotransmitter and postsynaptic receptor clustering in the hypoglossal nucleus. Mol. Cell. Neurosci. *32*, 254–273.

Nabekura, J., Katsurabayashi, S., Kakazu, Y., Shibata, S., Matsubara, A., Jinno, S., Mizoguchi, Y., Sasaki, A., and Ishibashi, H. (2004). Developmental switch from GABA to glycine release in single central synaptic terminals. Nat. Neurosci. *7*, 17–23.

Osen, K.K., Ottersen, O.P., and Storm-Mathisen, J. (1990). Colocalization of glycine-like and GABA-like immunoreactivities: a semiquantitative study of individual neurons in the dorsal cochlear nucleus of cat. In Glycine Neurotransmission, O.P. Ottersen and J. Storm-Mathisen, eds. (Hoboken, NJ: John Wiley), pp. 416–451.

Ostapoff, E.M., Benson, C.G., and Saint Marie, R.L. (1997). GABA- and glycine-immunoreactive projections from the superior olivary complex to the cochlear nucleus in guinea pig. J. Comp. Neurol. *381*, 500–512.

Overstreet, L.S., Westbrook, G.L., and Jones, M.V. (2002). Measuring and modeling the spatiotemporal profile of GABA at the synapse. In Transmembrane Transporters, M. Quick, ed. (New York: Wiley-Liss), pp. 259–276.

Pecka, M., Zahn, T.P., Saunier-Rebori, B., Siveke, I., Felmy, F., Wiegrebe, L., Klug, A., Pollak, G.D., and Grothe, B. (2007). Inhibiting the inhibition: a neuronal network for sound localization in reverberant environments. J. Neurosci. *27*, 1782–1790.

Raman, I.M., Zhang, S., and Trussell, L.O. (1994). Pathway-specific variants of AMPA receptors and their contribution to neuronal signaling. J. Neurosci. *14*, 4998–5010.

Renden, R., Taschenberger, H., Puente, N., Rusakov, D.A., Duvoisin, R., Wang, L.Y., Lehre, K.P., and von Gersdorff, H. (2005). Glutamate transporter studies reveal the pruning of metabotropic glutamate receptors and absence of AMPA receptor desensitization at mature calyx of held synapses. J. Neurosci. *25*, 8482–8497.

Rigo, J.M., Badiu, C.I., and Legendre, P. (2003). Heterogeneity of postsynaptic receptor occupancy fluctuations among glycinergic inhibitory synapses in the zebrafish hindbrain. J. Physiol. *553*, 819–832.

Riquelme, R., Saldana, E., Osen, K.K., Ottersen, O.P., and Merchan, M.A. (2001). Colocalization of GABA and glycine in the ventral nucleus of the lateral lemniscus in rat: an in situ hybridization and semiquantitative immunocytochemical study. J. Comp. Neurol. *432*, 409–424.

Rubio, M.E. (2006). Redistribution of synaptic AMPA receptors at glutamatergic synapses in the dorsal cochlear nucleus as an early response to cochlear ablation in rats. Hear. Res. *216–217*, 154–167.

Rubio, M.E., and Wenthold, R.J. (1997). Glutamate receptors are selectively targeted to postsynaptic sites in neurons. Neuron *18*, 939–950.

Rubio, M.E., and Juiz, J.M. (2004). Differential distribution of synaptic endings containing glutamate, glycine, and GABA in the rat dorsal cochlear nucleus. J. Comp. Neurol. *477*, 253–272.

Russier, M., Kopysova, I.L., Ankri, N., Ferrand, N., and Debanne, D. (2002). GABA and glycine co-release optimizes functional inhibition in rat brainstem motoneurons in vitro. J. Physiol. *541*, 123–137.

Sagné, C., El Mestikawy, S., Isambert, M.F., Hamon, M., Henry, J.P., Giros, B., and Gasnier, B. (1997). Cloning of a functional vesicular GABA and glycine transporter by screening of genome databases. FEBS Lett. *417*, 177–183.

Saint Marie, R.L., Benson, C.G., Ostapoff, E.M., and Morest, D.K. (1991). Glycine immunoreactive projections from the dorsal to the anteroventral cochlear nucleus. Hear. Res. *51*, 11–28.

Saint Marie, R.L., Shneiderman, A., and Stanforth, D.A. (1997). Patterns of gamma-aminobutyric acid and glycine immunoreactivities reflect structural and functional differences of the cat lateral lemniscal nuclei. J. Comp. Neurol. *389*, 264–276.

Shimamoto, K., Lebrun, B., Yasuda-Kamatani, Y., Sakaitani, M., Shigeri, Y., Yumoto, N., and Nakajima, T. (1998). DL-threo-beta-benzyloxyaspartate, a potent blocker of excitatory amino acid transporters. Mol. Pharmacol. *53*, 195–201.

Singer, J.H., and Berger, A.J. (1999). Contribution of single-channel properties to the time course and amplitude variance of quantal glycine currents recorded in rat motoneurons. J. Neurophysiol. *81*, 1608–1616.

Smart, T.G., Hosie, A.M., and Miller, P.S. (2004). Zn2+ ions: modulators of excitatory and inhibitory synaptic activity. Neuroscientist *10*, 432–442.

Spirou, G.A., and Berrebi, A.S. (1997). Glycine immunoreactivity in the lateral nucleus of the trapezoid body of the cat. J. Comp. Neurol. *383*, 473–488.

Suwa, H., Saint-Amant, L., Triller, A., Drapeau, P., and Legendre, P. (2001). High-affinity zinc potentiation of inhibitory postsynaptic glycinergic currents in the zebrafish hindbrain. J. Neurophysiol. *85*, 912–925.

Taschenberger, H., Leao, R.M., Rowland, K.C., Spirou, G.A., and von Gersdorff, H. (2002). Optimizing synaptic architecture and efficiency for high-frequency transmission. Neuron *36*, 1127–1143.

Todd, A.J., and Sullivan, A.C. (1990). Light microscope study of the coexistence of GABA-like and glycine-like immunoreactivities in the spinal cord of the rat. J. Comp. Neurol. *296*, 496–505.

Tollin, D.J. (2003). The lateral superior olive: a functional role in sound source localization. Neuroscientist *9*, 127–143.

Varoqui, H., Zhu, H., Yao, D., Ming, H., and Erickson, J.D. (2000). Cloning and functional identification of a neuronal glutamine transporter. J. Biol. Chem. *275*, 4049–4054.

Wenthold, R.J., and Hunter, C. (1990). Immunochemistry of glycine and glycine receptors in the central audutory system. In Glycine Neurotransmission, O.P. Ottersen and J. Storm-Mathisen, eds. (Hoboken, NJ: John Wiley), pp. 391–416.

Wenthold, R.J., Huie, D., Altschuler, R.A., and Reeks, K.A. (1987). Glycine immunoreactivity localized in the cochlear nucleus and superior olivary complex. Neuroscience *22*, 897–912.

Wojcik, S.M., Katsurabayashi, S., Guillemin, I., Friauf, E., Rosenmund, C., Brose, N., and Rhee, J.S. (2006). A shared vesicular carrier allows synaptic corelease of GABA and glycine. Neuron *50*, 575–587.

Wu, S.H., and Oertel, D. (1986). Inhibitory circuitry in the ventral cochlear nucleus is probably mediated by glycine. J. Neurosci. *6*, 2691–2706.

Zhang, W., Robert, A., Vogensen, S.B., and Howe, J.R. (2006). The relationship between agonist potency and AMPA receptor kinetics. Biophys. J. *91*, 1336–1346.